Unsteady Aerodynamic Responses of Mistuned Cascades to Incoming Wakes*
(Mistuning of Stagger Angle)

Ken-ichi FUNAZAKI**

Unsteady aerodynamic responses of a mistuned cascade subjected to incoming wakes from an upstream cascade are investigated in this study, where the extended Nishiyama-Funazaki method is employed. Numerical calculations are made, focussing on the effects of stagger angle mistuning of the cascade. It is accordingly found that there is some possibility of reducing wake-induced unsteady forces by controlling stagger angles without the severe expense of cascade performance deterioration. In addition, intense correlation between unsteady lifts and the corresponding steady lifts in the case of in-phase incoming wake conditions is observed.

Key Words: Unsteady Flow, Turbomachinery, Wake, Cascade, Wake Excitation, Blade Mistuning, Surface Singularity Method

1. Introduction

The mistuning technique of cascade airfoils in turbomachines has been eagerly studied as one of the possible ways to suppress undesirable blade vibration, e.g., flutter, or to reduce the noise level generated by rotor-stator potential interaction[1][2]. The mechanism of vibration or noise suppression is the interruption of periodicity in the tangential direction of the cascade by changing the natural frequency of each blade or by changing the cascade configuration, for example. Thus far, most of the concerns of the researchers have been limited to inviscid effect of the mistuning and very few studies have been conducted on wake interaction problems. In most cases, in spite of awareness of the importance of those problems, designers of turbomachines have been making efforts to prevent, for example, wake-induced resonance of the blade in a passive way by use of the Campbell diagram. In this sense, it seems useful to seek rather an active method of, for instance, blade mistuning adopted in this paper to avoid such problems or, at least, to reduce the

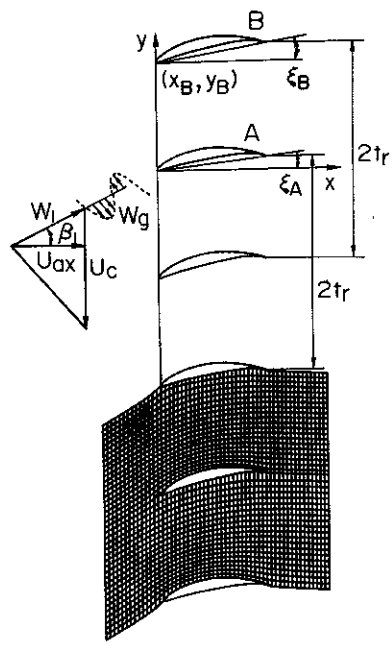

Fig. 1 Cascade configuration, inlet velocity triangle and computational grid for vorticity distribution

* Received 8th May, 1992. Paper No. 91-0031 B
** Department of Mechanical Engineering, Iwate University, 3-5 Ueda 4-chome, Morioka 020, Japan

severity to some extent.

The aim of this paper is then to investigate the effect of mistuning of the cascade configuration, especially the stagger angle, on the wake excitation forces acting upon the cascade airfoils. For this purpose, a prediction code was developed in this paper on the basis of the Nishiyama-Funazaki code[3], which was originally created for analysis of the wake-rotor interaction in normal cascades.

2. Mathematical Formulation

2.1 Steady flow

Flow is assumed to be two-dimensional, inviscid and incompressible. In this paper, a very simple case for the mistuning of the cascade is examined in which the cascade has alternating values of stagger angles between ξ_A and ξ_B in the tangential direction, as seen in Fig. 1. Of course, the method to be presented in the following can be easily extended to many ways of mistuning. Due to the linearity of the flow field, induced steady flow around the mistuned cascade of pitch t_r can be expressed by superposition of the solutions for two cascades with different stagger angles ξ_A and ξ_B, both of which have the same pitch $2t_r$ and are hereafter referred to as "cascade A" and "cascade B" respectively. Consequently, using the surface vorticity method, the so-called Martensen method[4], the steady velocity $(\bar{u}, \bar{v})$ induced on the airfoil surface of cascade A or B is given by Eq.(1).

$$(\bar{u}, \bar{v})=-\frac{\bar{\gamma}^C}{2}+\oint(g_x^A, g_y^A)\,\bar{\gamma}^A(s^A)ds^A+\oint(g_x^B, g_y^B)\,\bar{\gamma}^B(s^B)ds^B \quad (1)$$

$$g_x^C=-\frac{1}{4t_r}\frac{\sin(\pi(y-y')/t_r)}{\cosh(\pi(x-x')/t_r)-\cos(\pi(y-y')/t_r)}$$

$$g_y^C=\frac{1}{4t_r}\frac{\sinh(\pi(y-y')/t_r)}{\cosh(\pi(x-x')/t_r)-\cos(\pi(y-y')/t_r)} \quad (2)$$

where superscripts A and B mean the values associated with cascades A and B, respectively, and superscript C stands for each of them. Substituting Eq.(1) into the boundary condition on a airfoil surface,

$$\bar{\gamma}^C=(\bar{u}+\bar{u}_\infty)\frac{dx^C}{ds^C}+(\bar{v}+\bar{v}_\infty)\frac{dy^C}{ds^C} \quad (3)$$

one can obtain an integral equation for the surface vorticity strength $\bar{\gamma}^C$, where $(\bar{u}_\infty, \bar{v}_\infty)$ means vector-averaged flow. The obtained integral equation can be discretized by the trapezoidal rule along the airfoil surfaces with $2M$ pivotal points to obtain the following simultaneous equations for the solution vector, that is,

$$\bar{A}\bar{X}=\bar{B} \quad (4)$$

$$\bar{A}=\begin{pmatrix}\{\bar{A}^{AA}\}\{\bar{A}^{AB}\}\\ \{\bar{A}^{BA}\}\{\bar{A}^{BB}\}\end{pmatrix}\quad \bar{X}=\begin{pmatrix}\{\bar{\gamma}^A\}\\ \{\bar{\gamma}^B\}\end{pmatrix}\quad \bar{B}=\begin{pmatrix}\{\bar{B}^A\}\\ \{\bar{B}^B\}\end{pmatrix} \quad (5)$$

where a submatrix $\{\bar{A}^{IJ}\}$ with size $M\times M$ (I, J : A or B) represents influence coefficients from a cascade J to a cascade I. Equation (4) can be solved by the Gaussian elimination method in conjunction with Kutta conditions

$$\bar{\gamma}_1^A+\bar{\gamma}_M^A=0 \quad \bar{\gamma}_1^B+\bar{\gamma}_M^B=0 \quad (6)$$

to determine discretized surface vorticity distribution $(\bar{\gamma}^A, \bar{\gamma}^B)$. In this case, two possible ways to incorporate the Kutta conditions within the system equations (4) were examined. One method involves the substitution of the equations (6) with any two equations at proper pivotal points in the system equations. The other method involves the addition of the equations (6) to the system equations (4) so as to obtain new $2(M+1)$ system equations with $2M$ unknowns, and these can be solved by the least squares method. Comparing the results obtained by these two methods with the experimental data, it was found that the substitution method yielded better results than the least squares method, even though in the former case the discretized boundary conditions Eq.(3) were not fully satisfied over the airfoil surfaces. Therefore, the substitution method for the Kutta conditions is employed in this study.

Steady pressure coefficient $\bar{C}_p$, inlet flow angle to a mistuned cascade β_1 and outlet flow angle β_2 are calculated as follows:

$$\bar{C}_p=\frac{P_0-p}{1/2\rho U_{ax}^2}=\left(\frac{W}{W_1}\right)^2=\left(\frac{\bar{\gamma}}{W_1}\right)^2 \quad (7)$$

$$\beta_1=\tan^{-1}\left(\frac{\tan\beta_\infty-\Gamma/4t_r}{U_{ax}}\right)$$

$$\beta_2=\tan^{-1}\left(\frac{\tan\beta_\infty+\Gamma/4t_r}{U_{ax}}\right) \quad (8)$$

where β_∞ means vector-averaged flow angle to the mistuned cascade and Γ represents circulation along the closed path which includes two neighboring airfoils of cascade A and cascade B, and is given by summation of two circulations along the two airfoils,

$$\Gamma=\bar{\Gamma}^A+\bar{\Gamma}^B=\oint\bar{\gamma}^A ds^A+\oint\bar{\gamma}^B ds^B \quad (9)$$

2.2 Unsteady Flow

The original method[3] for wake-interaction problems in non mistuned cascades employs a unsteady velocity splitting technique by which unsteady velocity is split into an irrotational part (u^{IR}, v^{IR}) and a rotational part (u^R, v^R). The rotational part is directly associated with the vorticity originating from the incoming wakes and it is calculated by using the well-known relationship of stream function (ϕ^R)-vorticity (ζ), that is,

$$\nabla^2\phi^R=-(\zeta)$$

or its integral forms

$$u^R=-\frac{1}{2\pi}\iint_{-\infty}^{\infty}\frac{y-y'}{(x-x')^2+(y-y')^2}dx'dy'$$

$$v^R=\frac{1}{2\pi}\iint_{-\infty}^{\infty}\frac{x-x'}{(x-x')^2+(y-y')^2}dx'dy' \qquad (10)$$

To estimate the above integrals, the entire flow field is divided into three sub domains referred to as far-upstream, far-downstream and near-field. The integrals over the far-upstream and far-downstream domains are evaluated in an analytical manner, taking account of the uniformity of the steady flow there. On the other hand, the integrals over the near-field domain should be evaluated in a numerical manner. For this purpose, a grid system for computing the vorticity distribution and then the rotational velocity is introduced here in consideration of the tangential periodicity of the unsteady flow field with some phase shift (2σ). The grid system consists of several steady streamlines and vertical lines with equal axial spacing and it extends in the tangential direction between the two neighboring stagnation streamlines for cascade A as shown in Fig. 1. The contributions from the near-field domain to the rotational velocity, (u_n^R, v_n^R), are then calculated by the following equations.

$$u_n^R=-\frac{1}{2\pi}\iint_{\text{near-field}}\sum_{m=-\infty}^{\infty}\zeta e^{j2m\sigma}\times\frac{y-y'+2mt_r}{(x-x')^2+(y-y'+2mt_r)^2}dx'dy'$$

$$v_n^R=\frac{1}{2\pi}\iint_{\text{near-field}}\sum_{m=-\infty}^{\infty}\zeta e^{j2m\sigma}\times\frac{x-x'}{(x-x')^2+(y-y'+2mt_r)^2}dx'dy' \qquad (11)$$

Vorticity distribution within the grid system necessary for calculating Eq. (11) is then determined by the following equation,

$$\zeta_{IJ}=\zeta_{1J}\exp(-jk\Delta T_{IJ}) \quad \Delta T_{IJ}=\int^{S_{IJ}}\frac{d(s'/C)}{W(s')/U_{ax}} \qquad (12)$$

where subscript I and J mean an axial and a tangential position, respectively, and k is reduced frequency, which is defined by the following relationship.

$$k=\omega C/U_{ax}=\pi\frac{C}{t_r}\frac{t_r}{t_s}\frac{1}{\phi} \quad \phi: \text{flow coefficient} \qquad (13)$$

t_r/t_s is the rotor-stator, i.e., downstream-upstream cascade pitch ratio. It should be mentioned that Eq.(12) comes from the linearized vorticity transport equation without viscous effect, which means that the vorticity is assumed to be convected downstream along a steady streamline. Also note that the origin of the coordinate system is fixed on the leading edge of an airfoil of cascade A.

The Martensen method mentioned above is easily extended to the unsteady case to represent the unsteady irrotational velocity (u^{IR}, v^{IR}) by distributing unsteady surface vorticity (γ^A, γ^B) along the corresponding airfoil surfaces. With the use of the interblade phase angle of upstream wakes against the mistuned cascade, (2σ), (u^{IR}, v^{IR}) can be expressed as follows:

$$(u^{IR}, v^{IR})=-\frac{\gamma^C}{2}+\oint(F_x^A, F_y^A)\gamma^A(s^A)ds^A+\oint(F_x^B, F_y^B)\gamma^B(s^B)ds^B \qquad (14)$$

where

$F_x=f(\chi)+f(\bar{\chi}), \quad F_y=f(\chi)-f(\bar{\chi})$

$f(\chi)=\exp(j(\pi-2\sigma)\chi \text{ cosec } \pi\chi)$

$\chi=(y'-y+j(x-x'))/2t_r$

and the inter-blade phase angle (σ) between the two neighboring airfoils is given by

$$\sigma=2\pi\left(\frac{t_r}{t_s}-\text{int}\left[\frac{t_r}{t_s}\right]\right) \qquad (15)$$

int[x] : trancation function

Then, the unsteady boundary condition[5]

$$\gamma=(u^{IR}+u^R)\frac{dx}{ds}+(v^{IR}+v^R)\frac{dy}{ds} \qquad (16)$$

is specified on the airfoil surfaces, which requires that the tangential component of the unsteady velocity at a point on the surface is equal to the strength of the vorticity there. By substituting the rotational and irrotational velocities given by Eqs. (10) and (14) into the boundary condition, one can obtain the following integral equation for the surface unsteady vorticity strength γ:

$$-\frac{\gamma^C}{2}+\oint\{K_1(s^C, s'^A)+K_2(s^C)\}\gamma^A(s'^A)ds'^A+\oint\{K_1(s^C, s'^B)+K_2(s^C)\}\gamma^B(s'^B)ds'^B=-\left(u^R\frac{dx^C}{ds^C}+v^R\frac{dy^C}{ds^C}\right) \qquad (17)$$

where kernel function K_1 is related to the effect of the surface vorticity and kernel function K_2 means the effect of the vortices shed from the trailing edge of the airfoils. Readers who are interested in more information on these functions, are referred to the paper by Nishiyama and Funazaki[3]. In the same manner as in the steady flow case, Eq.(17) is discretized along the surfaces of cascades A and B with M pivotal points so as to obtain simultaneous equations similar to Eq. (4), and it is solved by the elimination method in conjunction with the unsteady Kutta condition which requires no loading at the trailing edge.

Consequently, unsteady pressure p, and then unsteady aerodynamic forces F_x, F_y and moment M around an axis (x_R, y_R) are calculated as

$$p(s)=-\rho\left[\bar{\gamma}(s)\gamma(s)+jk\int_{-\infty}^{s}\gamma(s')ds'\right] \qquad (18)$$

$$F_x=-\oint p(s)dy \quad F_y=\oint p(s)dx$$

$$M=\oint p(s)\{(x-x_R)dx+(y-y_R)dy\} \qquad (19)$$

and the corresponding unsteady pressure, lift and moment coefficients are respectively defined by

$$C_p=\frac{p}{\rho U_{ax}^2(W_g/U_{ax})}$$

$$C_L=\frac{L}{\rho U_{ax}^2(W_g/U_{ax})C} \quad C_M=\frac{M}{\rho U_{ax}^2(W_g/U_{ax})C^2} \tag{20}$$

where the unsteady lift is defined as,

$$L=-F_x\sin\xi+F_y\cos\xi, \quad \xi: \text{stagger angle} \tag{21}$$

3. Numerical Calculations

3.1 Problems

Figure 1 shows the configuration of the compressor cascade employed in the numerical calculations in this study. It consists of two types of cascades A and B with different configurations, i.e., stagger angles ($\xi^A=7°$ and $\xi^B=10°$), but with the same pitch $2t_r$ and airfoil section geometry, NACA 65(18)10[6]. Note that the level of this mistuning in stagger angle is adopted from an actual example in an aero-engine[1]. As mentioned earlier, the origin of the entire coordinate system coincides with that of cascade A shown in Fig. 1, and the origin of the local coordinate system for cascade B is set at the point (x_B, y_B). Hereafter, for simplicity, the case of $x_B=0$ and $y_B=t_r$ will be examined.

Before the discussion of parametric studies on the effect of the mistuning on the unsteady aerodynamic responses, some comments must be made on the types of parameters which will be used in this paper. Flow coefficient ϕ is chosen in a somewhat arbitrary manner to be 0.50. The pitch ratios t_r/t_s, in other words, blade number ratios N_s/N_r employed in this study are 0.50, 0.75, 1.00 and 1.25. It is also important to note that the reduced frequency k given by Eq.(13), as well as the interblade phase angle, Eq.(15), changes as the pitch ratio changes.

3.2 Check of accuracy of the code

For the purpose of checking the accuracy of the code presented above, steady and unsteady flow around a uniform or "tuned" cascade with stagger angle $\xi=7°$ and pitch $t_r/C=1$ are investigated by that code, and the results are compared with those of the original code for tuned cascades. As for the steady flow, it is verified that both codes yield almost the same results, which also agree very well with the experimental data.

Figure 2 shows a comparison between the results of the unsteady pressure difference along the chord in the case of $t_r/t_s=0.5$, where "Mistuned A" and "Mistuned B" indicate the results of neighboring airfoils in the tuned cascade with the spacing of $t_r/C=1$. Calculated amplitude distributions as well as phase distributions of the unsteady pressure difference along the actual chord for the tuned and mistuned cascades are almost identical, which confirms the validity of the code for the mistuned cascade. It should be noted that the phase difference between the airfoils of "Mistuned A" and "Mistuned B" should be 180° because $t_r/t_s=0.5$ (see Eq. (15)), and this requirement is well reproduced by the code, as shown in the figure.

3.3 Effect of Mistuning

3.3.1 Steady Flow Effects of stagger angle mistuning on the steady pressure distributions along the airfoils are examined, some numerical results being shown in Fig. 3 with the results for the tuned cascade for comparison. In addition, comparisons between the aerodynamic characteristics, axial/tangential fluid forces and moment, obtained for the tuned and mistuned cascades are listed in Table 1, where tuned B indicates the result for the uniform

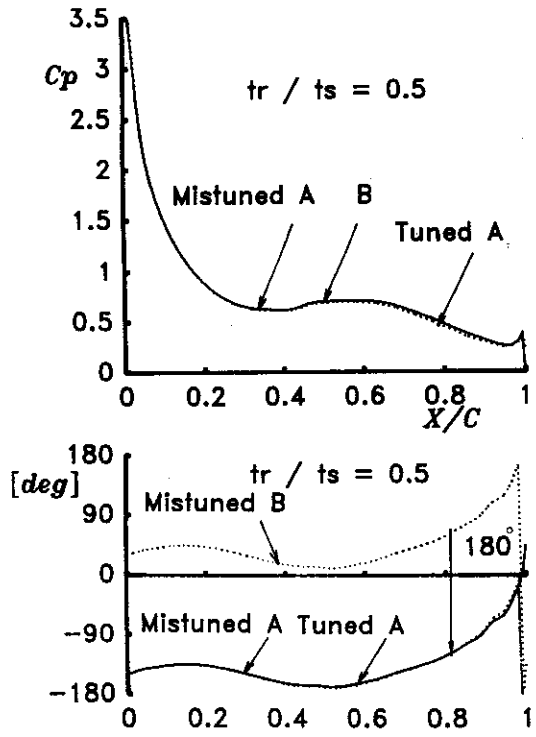

Fig. 2 Check of accuracy in the unsteady flow calculation

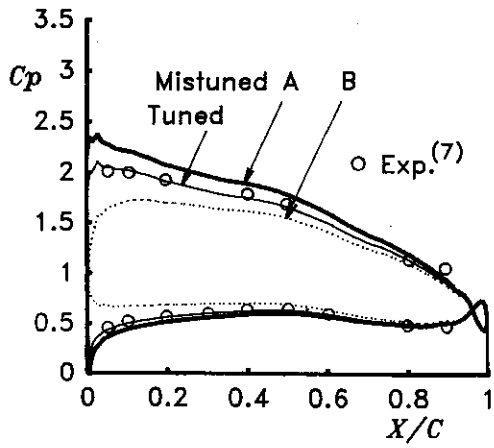

Fig. 3 Effect of mistuning on steady pressure distribution

cascade with stagger angle $\xi=10°$.

As seen in Fig. 3 or Table 1, steady loading of Mistuned A increases due to the stagger angle mistuning compared to that of "Tuned" in Fig. 3 or Tuned A in Table 1 which has the same stagger angle as Mistuned A, while the steady loading of the Mistuned B decreases compared to that of the Tuned or Tuned B in Table 1.

3.3.2 Unsteady Flow

(1) Unsteady pressure difference distribution

Figure 4 shows the unsteady pressure difference distributions of Mistuned A and Mistuned B in the case of $t_r/t_s=0.5$. A small difference in magnitude between the two results can be seen, although their profiles are almost the same. In the case of $t_r/t_s=1.0$ shown in Fig. 5, on the other hand, a salient difference between the results of Mistuned A and Mistuned B appears, where the amplitude of Mistuned B decreases markedly in comparison with that of Mistuned A. The reason for this difference is presumed to be as follows: The interblade phase angle between Mistuned A and Mistuned B is zero and the unsteady aerodynamic interaction between the airfoils becomes relatively weak in this case as if each airfoil of the cascade were behaving like an isolated airfoil; hence the effect of the change in steady loading upon the unsteady characteristics becomes noticeable in a rather straightforward way.

Since the results in these figures also include the effect of local flow angle, i.e., incidence to the airfoils, however, such comparisons in Figs. 4 and 5 do not seem to be sufficient for understanding aerodynamic aspects of the mistuning effect. Therefore, to investigate that effect in further detail, it might be convenient to compare the results obtained for the airfoils in the mistuned and tuned cascades with the same stagger angle for different pitch ratios, which results are shown in Figs. 6 - 11 described by the notations "Mistuned A-Tuned A" or "Mistuned B-Tuned B". Figures 6 and 9 for the case of $t_r/t_s=0.5$ show that the amplitude distributions for the mistuned airfoils are slightly smaller than those of the tuned airfoils, and the mistuning does not seem to have any considerable effect on the unsteady aerodynamic characteristics in this case. On the other hand, in Figs. 7 and 10 for the case of $t_r/t_s=1.0$, the mistuning effect becomes prominent so that the profiles of pressure difference distributions for the tuned and mistuned airfoils differ considerably, especially between Mistuned A and

Table 1 Steady aerodynamic characteristics of the tuned and mistuned cascade

	$\xi°$	$\beta_2°$	C_{FX}	C_{FY}	C_M
Mistuned A	7	-2.01	-0.411	1.485	0.536
Mistuned B	10	-2.01	-0.266	0.967	0.635
Tuned A	7	-3.44	-0.334	1.273	0.469
Tuned B	10	-0.40	-0.339	1.169	0.450

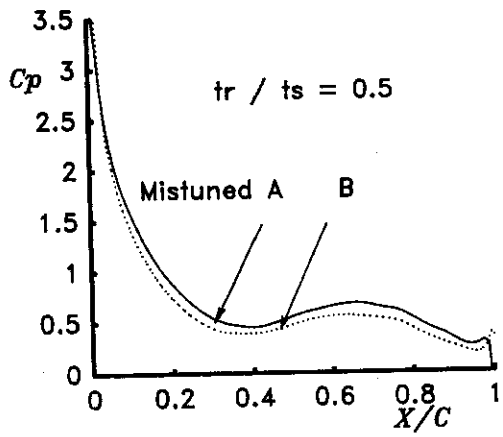

Fig. 4 Unsteady pressure difference along the blade chord ($t_r/t_s=0.5$)

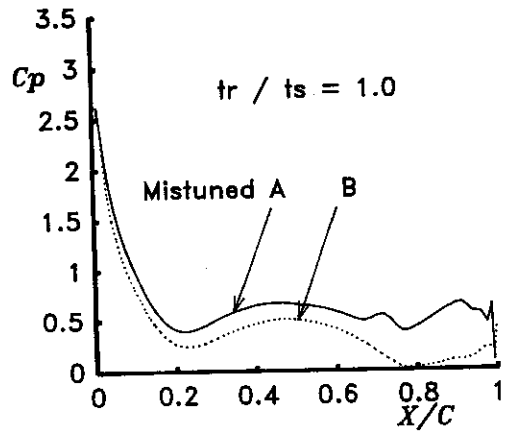

Fig. 5 Unsteady pressure difference along the blade chord ($t_r/t_r=1.0$)

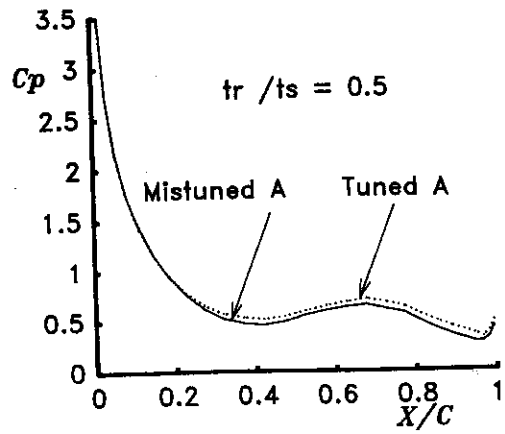

Fig. 6 Comparison of unsteady pressure differences for tuned cascade A and mistuned cascade A ($t_r/t_r=0.5$)

Tuned A. This is almost the case for $t_r/t_s=1.25$ in Figs. 8 and 11.

(2) Unsteady Lift and Moment

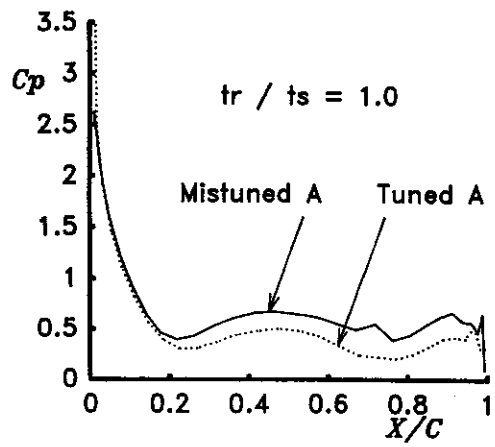

Fig. 7 Comparison of unsteady pressure difference for tuned cascade A and mistuned cascade A ($t_r/t_r=1.0$)

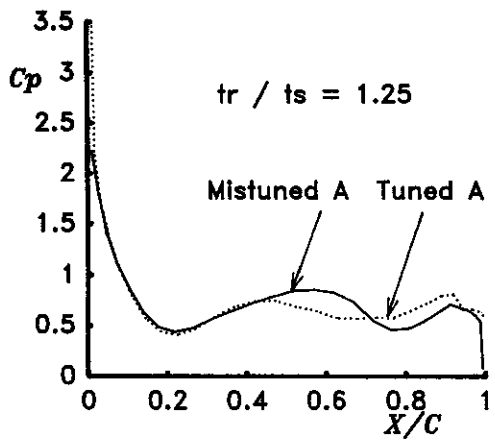

Fig. 8 Comparison of unsteady pressure differences for tuned cascade A and mistuned cascade A ($t_r/t_s=1.25$)

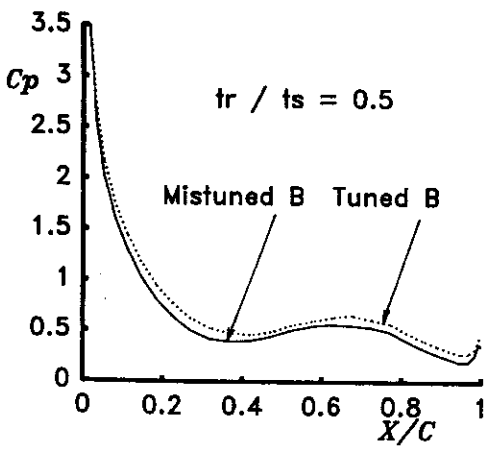

Fig. 9 Comparison of unsteady pressure differences for tuned cascade B and mistuned cascade B ($t_r/t_s=0.5$)

As mentioned above, the levels of the mistuning effect on the unsteady aerodynamic characteristics of the mistuned cascade vary with the pitch ratio t_r/t_s, the case for which is reconsidered in terms of the unsteady lift and moment in Figs. 12 and 14. Figure 12 shows several curves of unsteady lift coefficient C_L versus pitch ratio t_r/t_s. From this figure, one may easily note that there arises a relatively large difference among those curves at $t_r/t_s=1.0$, which is to be examined in the following.

Figure 13 shows curves for C_L/C_{L0}, the reduced unsteady lift coefficients divided by the corresponding steady lift coefficients, with respect to the pitch ratio. The author would like to stress an interesting phenomenon in this figure in which all calculated data values at $t_r/t_s=1.0$ tend to coincide with each other. This coincidence does not occur by chance. On the contrary, it indicates that the rate of change in magnitude of the unsteady lift coefficient due to the change in stagger angle is almost proportional to that

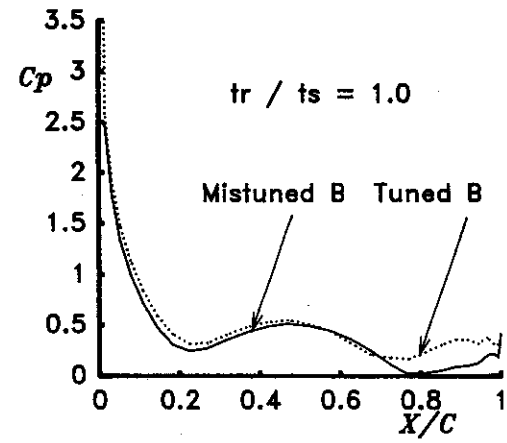

Fig. 10 Comparison of unsteady pressure differences for tuned cascade B and mistuned cascade B ($t_r/t_s=1.0$)

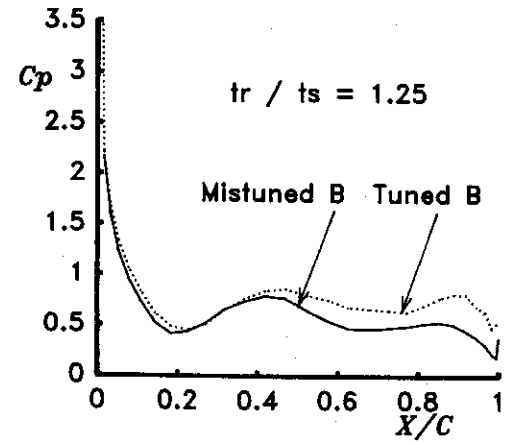

Fig. 11 Comparison of unsteady pressure differences for tuned cascade B and mistuned cascade B ($t_r/t_s=1.25$)

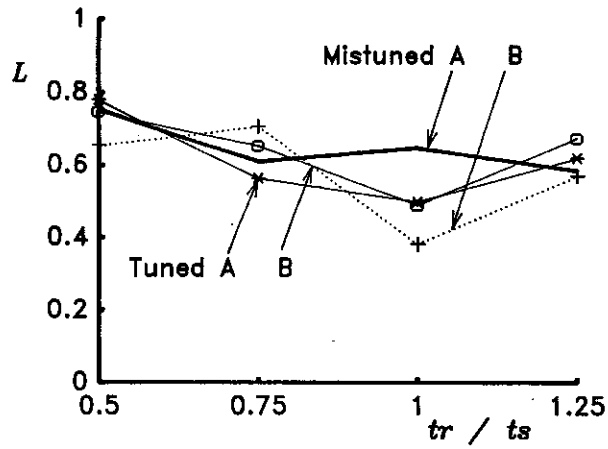

Fig. 12 Variation of unsteady lift coefficient with respect to the pitch ratio t_r/t_s

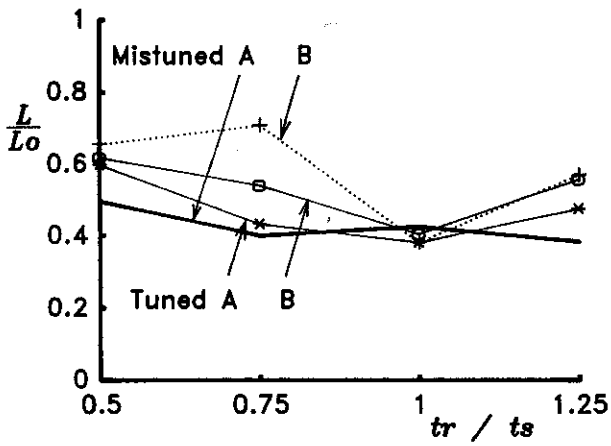

Fig. 13 Variation of the reduced unsteady lift coefficient by the corresponding steady lift with respect to the pitch ratio t_r/t_s

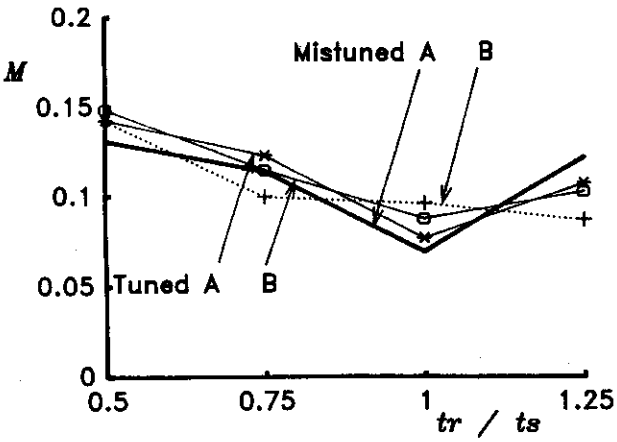

Fig. 14 Variation of unsteady moment coefficient with respect to the pitch ratio t_r/t_s

of change in the corresponding steady lift coefficient. In other words, in the case of $t_r/t_s=1.0$ in which the interblade phase angle is zero between the neighboring airfoils, unsteady aerodynamic characteristics of the tuned or mistuned cascade could be approximately estimated with the corresponding steady characteristics multiplied by a factor, although such a factor can rarely be determined a priori. The author does not have enough data to generalize the above discussion at this moment, so it is clear that there is much room for further investigation.

Except for the case of $t_r/t_s=1.0$, due to the blade-to-blade aerodynamic interaction, marked correlation between the rates of change in steady and unsteady lift coefficients does not seem to exist any more. Moreover, "Mistuned *B*" in the mistuned cascade tends to have larger values of the unsteady lift coefficient than "Mistuned *A*".

From the curve of the unsteady lift coefficients in Fig. 12 around $t_r/t_s=1.25$, it is also found that magnitudes of the unsteady lifts slightly decrease due to the mistuning compared to those of the tuned cascades, which implies some possibility of reducing wake excitation forces with proper mistuning. Also, as for the unsteady moment acting on the mistuned cascade, Fig. 14 shows that reducing its value could be achieved by proper mistuning.

4. Conclusions

Wake excitation forces of the cascade which was "mistuned" so as to have alternating stagger angles in the tangential direction were analyzed by the method presented in this paper, and the following conclusions were obtained:

1. Stagger-mistuning affected unsteady aerodynamic characteristics considerably, and the level of that effect depended on the rotor-stator pitch ratio.
2. There were some possible conditions at which induced unsteady lift or moment acting on the cascade airfoils could be reduced.
3. Strong correlation between unsteady lift and the corresponding steady lift in the case of $t_r/t_s=1.0$, in-phase incoming condition of the wake, was observed; therefore in that case it might be possible to predict unsteady aerodynamic characteristics of the cascade by the corresponding steady characteristics to some extent.

Acknowledgements

The author is grateful for support from Mr. Toru Iwasaka, ex-undergraduate student of Iwate University, in numerical calculations.

References

(1) Kodama, H. and Nagano, S., Potential Pressure Field by Stator/Downstream Strut Interaction, ASME Paper 88-GT-54(1988).
(2) Bendiksen, O. O., Recent Developments in Flutter

Suppression Techniques for Turbomachinery Rotors, J. Propulsion, Vol. 4, No. 2(1988), p. 164.
(3) Nishiyama, T. and Funazaki, K., Aerodynamic Responses of Turbine Rotor Blade to Sinusoidal Gust of Large Vorticity, Trans. Jpn. Soc. Mech. Eng. (in Japanese), Vol. 50, No. 454, B(1984), p. 1476.
(4) Lewis, R. I., Vortex Element Methods for Fluid Dynamic Analysis of Engineering Systems, Cambridge University Press(1991), p. 75.
(5) Nishiyama, T. and Yanome, M., Aerodynamic Responses of Turbine Rotor Blades to Sinusoidal Gust, Trans. Jpn. Soc. Mech. Eng. (in Japanese), Vol. 45, No. 394, B(1979), p. 763.
(6) Emery, J. C., Herrig, L. J., Erwin, J. R. and Felix, A. R., Systematic Two-Dimensional Cascade Tests of NACA 65-Series Compressor Blades at Low Speed, NACA Technical Report 1368(1957).